A Study on the Modeling of Transitional Lateral Force Acting on the Berthing Ship by CFD

Gil-Young Kong*, Yun-Sok Lee, Sang-Min Lee
Department of Ship Operation System Engineering, Korea Maritime University, 1 Dongsam-dong, Yeongdo-gu, Busan 606-791 Korea

To evaluate the unsteady motion in laterally berthing maneuver, it is necessary to estimate clearly the magnitudes and properties of hydrodynamic forces acting on ship hull in shallow water. A numerical simulation has been performed to investigate quantitatively the hydrodynamic force according to water depth for Wigley model using the CFD (Computational Fluid Dynamics) technique. By comparing the computational results with the experimental ones, the validity of the CFD method was verified. The numerical solutions successfully captured some features of transient flow around the berthing ship. The transitional lateral force in a state ranging from the rest to the uniform motion is modeled by using the concept of circulation.

Key Words : Berthing Ships, Hydrodynamic Force, Transitional Lateral Force, SGS Model, CFD, Shallow Water

1. Introduction

The berthing maneuver is a specific work that should keep the allowance strength of the mooring facilities as well as the safety of the berthing ship itself. The accurate position and control of the vessel are required in addition to the aid of tugboats. One of the problems in a berthing maneuver is that the magnitude and features of the hydrodynamic force acting on ship hull as a function of water depths and ship types have not been analyzed clearly. In typical berthing motion of a large tanker vessel, the berthing maneuver is usually executed in low lateral moving velocity and in the short distance to the berth. The considerable force will act on ship hull because it is not a streamlined form to themoving direction. In such motion, the transitional lateral force is subject to the position and strength of the separated vortices. Moreover since the hydrodynamic forces differ greatly according to their kinetic history even in the same velocity, the force cannot be dealt with steady or quasi-steady condition. The transitional lateral force presents itself strongly, and remains for a very long time especially in the shallow water.

It is assumed that the hydrodynamic force can be simply divided into inertia force and lateral force. Concerning with the inertia force such as added mass, Lee et al.(2000) already proposed the simplified equations expressed with the water depth and the type of ships. With lateral force, Sadakane et al.(1996) has conducted a model experiment, and suggested an estimation formula based on the experiment results. However, it is required the hydrodynamic comprehension concerning the mechanisms of the hydrodynamic force. In recent years, Chen et al.(1993, 1996) have carried out using the chimera RANS method for the time domain simulation. It has been demonstrated that the feasibility and validations of RANS method for berthing ship. However, the hydrodynamic forces which works on a ship hull

* Corresponding Author,
E-mail : kong@hhu.ac.kr
TEL : +82-51-410-4273; **FAX** : +82-51-405-3402
Department of Ship Operation System Engineering, Korea Maritime University, 1 Dongsam-dong, Yeongdo-gu, Busan 606-791 Korea. (Manuscript **Received** November 14, 2003; **Revised** April 26, 2004)

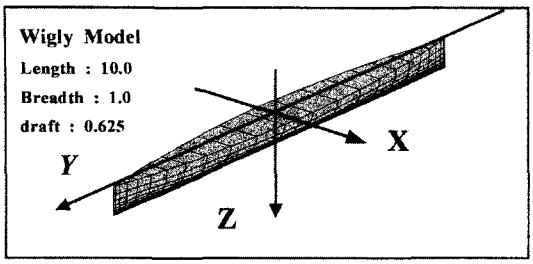

Fig. 1 Coordinate system and computational grid

are not shown in their research.

In this study, CFD (Computational Fluid Dynamics) have been performed for a Wigley model in laterally berthing motion to investigate the hydrodynamic force quantitatively and to visually observe the detailed characteristics of the flow field. The model experiments are carried out to evaluate the validity of CFD method. This paper presents the change of transitional lateral drag force according to the water depths and a model predicting the lateral force based on the computed results using the concept of circulation practically.

2. Outline of Numerical Method

The berthing velocity of a large tanker aided by tugboat operation in harbor is usually less than 0.15 m/s, and the Froude Number determined by taking the ship breadth is very small values. Based upon these facts, influence of the free surface was neglected in the computation. The motion mode during the lateral moving used for computation corresponds to CAT (Constant Acceleration Test) starting from rest to constant acceleration, to uniform movement, to constant deceleration, and to stop.

2.1 Governing equation and turbulence model

The governing equations are the continuity and Naiver-Stokes equations for viscous incompressible flow written in a physical domain using the Cartesian coordinate fixed on ship hull. All the variables are normalized by means of B, U_0, ρ and combination of these factors. where B is the ship breadth, U_0 the lateral moving velocity and ρ is the fluid density. The non-dimensional equations are transformed for the computational domain in non-orthogonal curvilinear coordinate. A partial transformation is used in which only the independent variables are transformed. Each equation is generally rewritten in the form of the convection/diffusion equation as follow ;

$$\frac{1}{J}\sum_{i=1}^{3}\sum_{j=1}^{3}\frac{\partial}{\partial\xi^i}(b_i^j U_j)=0 \tag{1}$$

$$\sum_{i=1}^{3}\sum_{j=1}^{3}g^{ij}\frac{\partial^2\phi}{\partial\xi^i\partial\xi^j}-2\sum_{j=1}^{3}a_\phi^j\frac{\partial\phi}{\partial\xi^j}=R_{eff}\frac{\partial\phi}{\partial\tau}+S_\phi \tag{2}$$

where b_i^j, g^{ij} and J represent the geometric coefficients, components of the conjugate metric tensor and Jacobian. Further details of the variables has been given in Patel et al.(1990). R_{eff} is the effective Reynolds number defined as $\frac{1}{R_{eff}}=\frac{1}{R_e}+\nu_t$, where R_e is the Reynolds number and ν_t is the eddy viscosity. The SGS (Sub-Grid Scale) model is employed for the turbulent flow. The validity of SGS model using the Smagorinsky et al.(1965) assumption for the eddy viscosity was provided by Miyata et al. (1992). This model seems to be more versatile properties for capturing the characteristics of unsteady and a separated flow around the berthing ship, having simple equations and relatively rough computational grids. The eddy viscosity, ν_t can be solved using the Takakura's length scale (Takakura et al. 1989) as follows ;

$$\nu_t=L_s^2(2\overline{e^{ij}}\ \overline{e^{ij}})^{1/2} \tag{3}$$

where the Takakura's length scale, L_s is given as ;

$$L_s=0.5\min(\Delta\xi, \Delta\eta, \Delta\zeta) \tag{4}$$

and e^{ij} represents the contravariant components of the strain tensor. $\Delta\xi$, $\Delta\eta$, $\Delta\zeta$ are the minimum space of computational girds.

The transport equations are discretized using the 12 point finite analytic method (Patel et al., 1990; Tahara, 1993). In the finite-analytic scheme, the equation is linearlized in each local numerical elements and solving analytically by the method of separation of variables. The Euler

implicitq method is applied to the time derivatives. Pressure-velocity coupling is accomplished using the PISO algorithm (Chen et al., 1993). Therefore hundred times of repetition is required for every trial for the calculation of one-time step, the coefficient of the FA method was renewed each time repetition.

2.2 Computational grid and boundary conditions

The present computational grid is H-type with constant Y planes, which is generated by solving the Possion equation. The coordinate system and computational grid of Wigley hull are shown in Fig. 1. The origin is at the water surface of midship section. X is the opposite direction for the movement, Y is the ship length direction and Z is directed vertically downward. Ship's length and draft are normalized by breadth. Therefore the length is 10, breadth is 1.0, and draft is 0.625. The number of computational girds is $81\times95\times35$ in directions of X, Y, and Z in case of the deep water region. In case that water depth-draft ratio, H/d is 2.0 and 1.5, computation was conducted by reducing exclusively the number of Z direction grids to 19 and 21, respectively. Figure 2 shows the computational gird on the water surface plane. The boundary condition are given in the shallow water region as follows: the inlet boundary condition ($X=-30$); $u=U_0$, $v=w=p=0$, the outlet boundary condition ($X=30$); $\partial u/\partial x=\partial v/\partial x=\partial w/\partial x=\partial p/\partial x=0$, the side (right and left) boundary condition ($Y=\pm25$); $u=U_0$, $v=w=p=0$. Furthermore the boundary condition on the hull surface was approximated with $v=w=p=0$, $\partial p/\partial x=dU_0/dt$. The body hull is located $-5\leq Y\leq5$, $-0.5\leq X\leq0.5$. Non-dimensional acceleration and deceleration for computation is ±1 ($dU_0/dt=\pm1$). The Reynolds number was designated as 10^5 considering the Reynolds number of the experiment, and the non-dimensional time interval of 1 step, Δt is 0.005 (200 steps are equivalent to the non-dimensional time, T=1.0).

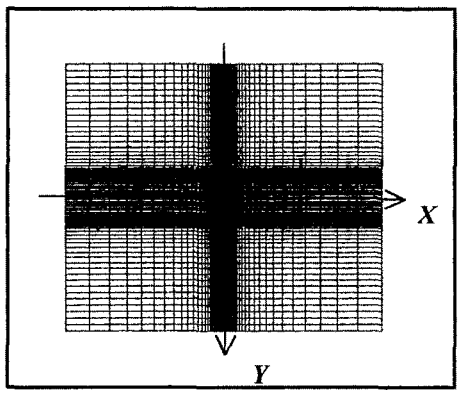

Fig. 2 Computational grid on the water plane

3. Numerical Results

3.1 Change in the hydrodynamic force according to water depth

The comparison of the hydrodynamic force between the computations and experiments according to the water depth-draft ratio H/d, such as H/d=2.0, 1.5 and H/d=7.0 is shown in Fig. 3. The force, F and lateral moving velocity, U_0 in Fig. 3 are the normalized values, and the non-dimensional acceleration is 1.0. The solid line gives the computation result, whereas the dotted line gives the experimental results. In order to compare both of the hydrodynamic forces directly, inertia force corresponding to the model mass used in the experiment was added to the CFD results. The experimental result in Fig. 3 is obtained by means of lateral force measurement equipment using a servo motor control, as shown in Fig. 4. The equipment can move the experimental model within 1.0 m, and the carriage speed and the acceleration are set on the personal computer. It is shown that the CFD result is satis-

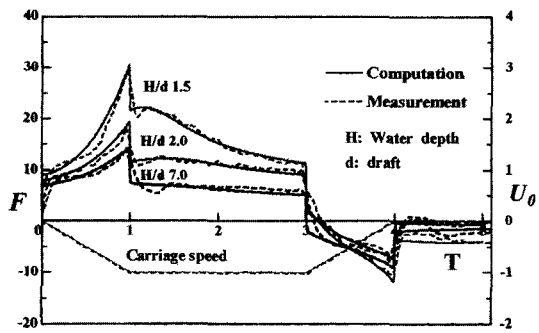

Fig. 3 Comparison of hydrodynamic forces

factory enough to coincide with the experimental result. Thus it is validated that the hydrodynamic force obtained from the CFD method can be estimated with sufficient accuracy. Also, the force in Fig. 3 is almost pressure component, and the viscosity stress component is small enough to be ignored. As a feature of the hydrodynamic force caused by the difference of water depth, especially the transitional lateral force under uniform movement is showed largely as the force comes to more shallow water. Furthermore a feature came to manifest itself remarkably with decrease of the force in a short time. The added mass concerning the inertia component appearing just after acceleration and just before deceleration was found to be almost the same in its magnitude despite the great difference of the flow field around the ship. Also utilizing the merit of CFD computation, change of the flow field dependent on water depth is hereby observed. Instantaneous streamlines of water surface plane in case that H/d=2.0 and 1.5 are shown in Fig. 5. Since the flow comes to

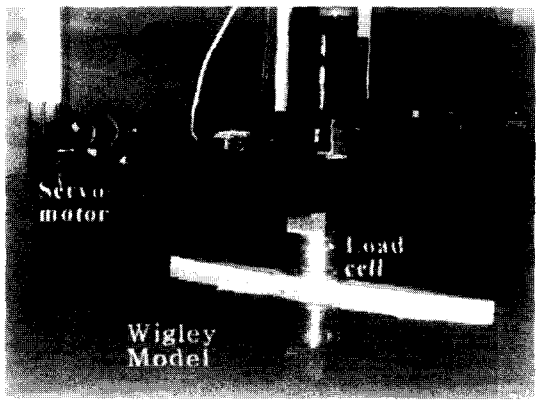

Fig. 4 Configuration of experiment

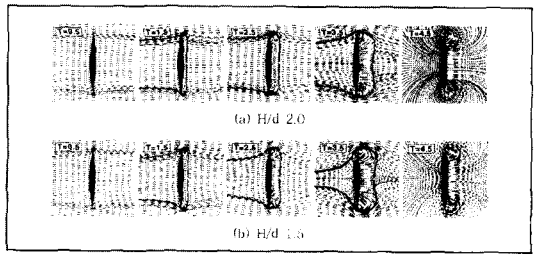

Fig. 5 Instantaneous streamlines of water surface (relative velocity to the hull)

be hard to go through the ship bottom, a flow running around the fore and aft makes remarkable appearance in shallow water. Therefore it is shown that great positive pressure is worked on the front of the hull in a shallow region. From the visualized information, the influence on the flow field around the ship hull can very easily be explained. Thus it can be ensured that the water depth is an important element to affect in fluence on the hydrodynamic force, and it has become possible to compare and examine the hydrodynamic force in detail based on the CFD computation result.

3.2 Change in the hydrodynamic force according to the acceleration

In undergoing laterally berthing maneuver, the ship makes lateral moving with the support of a tugboat, but acceleration movement is made with the hull from rest to uniform movement. Thus change of the flow field influenced by the difference of acceleration movement depending on the number of the tugboat and the power of the tugboat is hereby examined. Even if the lateral moving velocity is the same, it is considered that the hydrodynamic forces acting on ship hull according to the difference of acceleration is greatly different. To examine the change of the hydrodynamic force effected by the difference of the acceleration, computation was made from rest to uniform movement T=5.0 using the CFD method in case that H/d=7.0 where the water depth is deep enough and H/d=1.5 where the water depth is relatively shallow taking up the 3 types of different non-dimensional acceleration (i.e., NDA 0.5, 1.0, and 2.0). Computational results of the hydrodynamic forces according to the acceleration is compared with experiment result in Fig. 6 (H/d=7.0) and Fig. 7 (H/d=1.5), respectively. From the Figs. 6 and 7, it is confirmed that the CFD results is in coincidence with the experiment with good accuracy. Thus it might be possible to evaluate the hydrodynamic force by the use of CFD.

Let the hydrodynamic force under the lateral moving of the ship hull can be classified into inertia force and lateral force. The inertia force

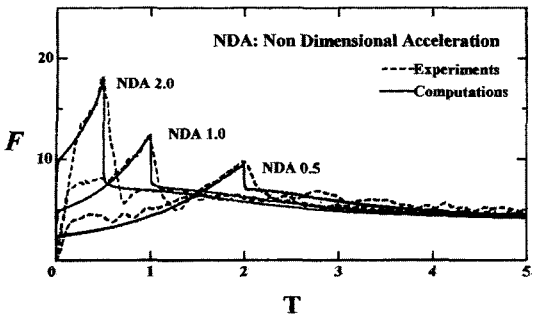

Fig. 6 Comparison of hydrodynamic forces according to the acceleration (H/d=7.0)

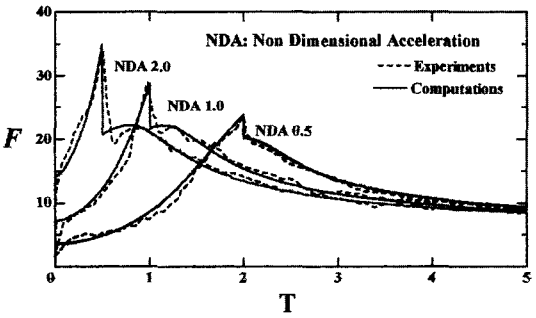

Fig. 7 Comparison of hydrodynamic forces according to the acceleration (H/d=1.5)

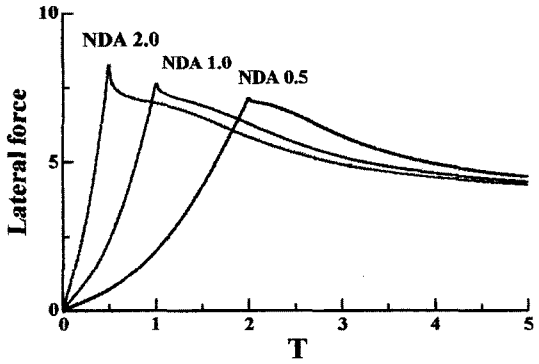

Fig. 8 Comparison of lateral drag force (H/d=7.0)

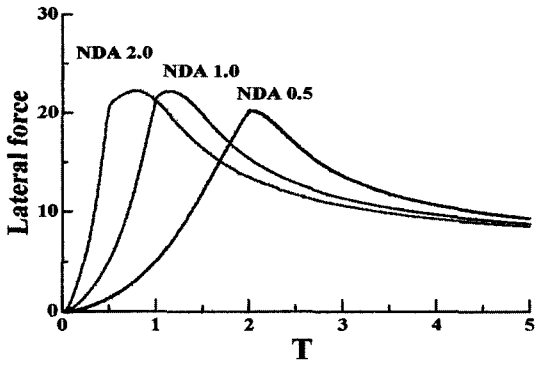

Fig. 9 Comparison of lateral drag force (H/d=1.5)

in case that NDA is 2.0 was twice as large as the force in case that NDA is 1.0. The inertia force in case that NDA is 0.5 was half of the one referred to above. In case that NDA is 1.0, the inertia force in a deep water H/d=7.0 was 4.8, whereas the value was 7.2 in a shallow H/d=1.5. Thus it is ensured that among the hydrodynamic forces subjected to the difference of the acceleration, the inertia force becomes larger which is dependent exclusively on the acceleration.

The lateral force obtained by deducting inertia force from computational results of the CFD is shown in Figs. 8 and 9. Comparing Fig. 8 with Fig. 9, the lateral force becomes approximately 3 times larger at H/d=1.5 than at H/d=7.0 and is greatly susceptible to the influence of the shallow water. Meanwhile as long as the water depth was the same, almost none of difference was noticed with the maximum value (just after acceleration) caused by the difference of the acceleration. However the tendency of transitional lateral force was slightly different. In case that the water depth is shallow (H/d=1.5), the lateral force was increased for a while just after starting the uniform movement. Such features remarkably appeared when the acceleration is very high.

4. Modeling of Lateral Drag Force

The lateral force ranging from a resting state to uniform movement is aligned according to the lateral moving distance of the hull based on a report by Sadakane et al.(1996). Details of the above are shown in Fig. 10 (H/d=7.0) and Fig. 11 (H/d=1.5). The abscissa of both the figures correspond to the lateral moving distance S, whereas the ordinate comply with the coefficients of transitional lateral force. The coefficients of transitional lateral force, C_{wy} is defined as $C_{wy}=F/0.5\rho LdU_0$. First in case of Fig. 10 indicating the deep water, slight difference is noted, but totally good agreement is seen. However in case of H/d=1.5 where the water depth is relatively

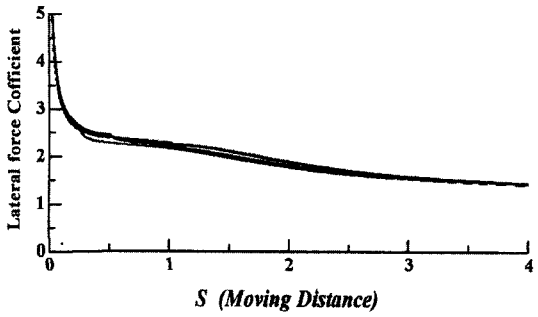

Fig. 10 Lateral drag coefficient according to the moving distance when H/d=7.0

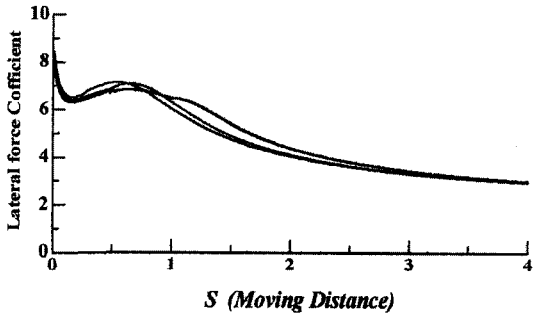

Fig. 11 Lateral drag coefficient according to the moving distance when H/d=1.5

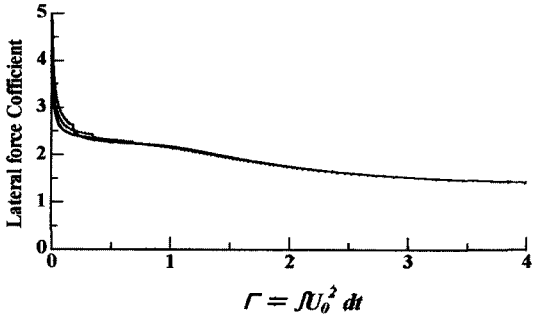

Fig. 12 Lateral drag coefficient according to the circulation when H/d=7.0

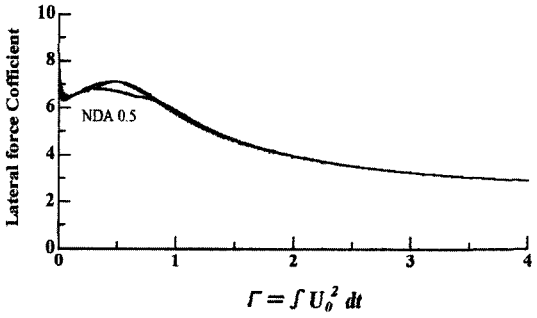

Fig. 13 Lateral drag coefficient according to the circulation when H/d=1.5

shallow, the tendency is quite different from the one in case of the deep water. Especially in case that $S<3.0$, disagreement is noted. That is to say, it is almost impossible to align the lateral force by means of exclusively the lateral moving distance.

As a method to express the transitional lateral force quantitatively, modeling of the transitional lateral force coefficient is attempted by introducing the concept of circulation as a variable closely related with the magnitude and development of the vortex surrounding the hull. From the fact that the velocity of the separated vortex is in proportion to the lateral moving velocity of the hull, the function of circulation is expressed using the lateral moving velocity and moving distance as follows:

$$\Gamma=\int u ds \propto U_0^2\, dt \qquad (5)$$

The coefficient of transitional lateral force obtained by taking the Eq. (5) is shown in Figs. 12 and 13. They comply with the lateral coefficient in case that H/d is 7.0 and 1.5, respectively. Comparing Figs. 12 and 13 with Figs. 10 and 11, it is found that it is possible to use circulation in case of both the deep water and the shallow water. However in case of the shallow water as shown in Fig. 13, the one exclusively with NDA 0.5 becomes smaller than the other ones in the vicinity of $S=0.5$. Using the circulation obtained by multiplying the lateral moving velocity of the hull with its moving distance, it is considered that modeling of the lateral force coefficient ranging from a resting state to uniform movement becomes possible. Investigation for modeling to describe the transitional lateral force coefficient of real ship except Wigley is required.

5. Conclusion

By applying the 3-dimensional CFD method to a Wigley hull, unsteady hydrodynamic force acting on a berthing ship was calculated. The most important conclusions of this paper are as

follows :

(1) The CFD computation result is in good agreement with the experimental result, and it is found that the unsteady hydrodynamic force under the laterally berthing maneuver can be estimated with good accuracy by the CFD technique.

(2) It is found that water depth is an important factor to make influence on the inertia force and transitional lateral force acting on ship hull.

(3) The added mass in case of acceleration and deceleration is almost of the same magnitude despite the difference of fluid field surrounding the hull.

(4) The transitional lateral force in a state ranging from the rest to the uniform motion is modeled by using the concept of circulation, which is obtained by multiplication of the lateral moving distance and moving velocity.

These results will be utilized to enhance the safety of berthing operation, to improve the ship-handling simulators and to design the strength of berthing facilities and fender systems, etc.

Acknowledgment

This work was supported by Korea Sea Grant Program 2003 of the Ministry Affairs and Fisheries, Korea.

References

Chen, H. C. and Korpus, R., 1993, "A Multiblock Finite-Analytic Reynolds-Averaged Navier-Stokes Method for 3D Incompressible Flows," *Individual Papers in Fluid Engineering, edited b F. M. White*, ASME FED-Vol. 150, *ASME Fluids Engineering Conference*, pp. 113~121.

Chen, M. and Chen, H. C., 1996, "Numerical Simulation of Transitional Flows Induced by a Berthing Ship," *International Journal of Offshore and Polar Engineering*, ISOPE, Vol. 7, No. 4, pp. 277~284.

Lee, Y. S., Sadakane, H. and Toda, Y., 2000, "Hydrodynamic Forces Acting on a Ship Hull Under Lateral Low Speed Motion," *Journal of the Japan Institute of Navigation*, No. 102, pp. 87~95.

Miyata, H., Zhu, M. and Watanabe, O., 1992, "Numerical Study on a Viscous Flow with Free-Surface Water about a Ship in Steady Course by a Finite-Volume Method," *Journal of Ship Research*, Vol. 36, No. 4, pp. 332~345.

Patel, V. C, Chen, H. C. and Ju, S., 1990, "Ship Stern and Wake Flows : Solutions of the Fully-Elliptic Reynolds-Averaged Navier-Stokes Equations and Comparisons with Experiments," *Journal of Computational Physics*, Vol. 88, No. 2, pp. 305~336.

Smagoriksky, J., Manabe, S. and Hollowya, J. L., 1965, "Numerical Results Form a Nine-Level General Circulation Model of the Atmosphere," *Monthly Weather Review*, Vol. 93, pp. 727~768.

Sadakane, H., 1996, "A Study on Lateral Drag Coefficient for Ship Moving Laterally from Rest," *Journal of the Japan Institute of Navigation*, No. 95, pp. 193~200.

Tahara, Y., 1993, "Computation of Viscous Flow around Series 60 Model and Comparison with Experiments," *Journal of The Kansai Society of Naval Architects*, No. 220, pp. 29~47.

Takakura, Y., Ogiwara, S. and Isiguro, T., 1989, "Turbulence Models for Transonic Viscos Flow," *AIAA paper*, 89-1952 CP.